Proton Damage in Advanced Laser Diodes

A. H. Johnston, *Sr. Member IEEE*, T. F. Miyahira and B. G. Rax

***Abstract* - Proton radiation damage in laser diodes is investigated for several types of laser diodes with wavelengths from 650 to 1550 nm. Key parameters include slope efficiency, threshold current, and the transition characteristics between LED and laser operation. Some of the devices exhibited nonlinear relationships between threshold current and proton fluence. All of the lasers, including VCSELs, were strongly affected by recombination-enhanced annealing, in contrast to double-heterojunction LEDs, which are only slightly affected by annealing. Analysis of laser characteristics after irradiation showed that the main effect of radiation damage is an increase in bulk recombination that increases loss within the laser cavity**

I. Introduction

Many advances have been made in laser diodes that have extended the wavelength range over which semiconductor lasers can be used, and also reduced the threshold current required for operation. Key technical advances include the use of thin heterostructures that allow efficient carrier injection over dimensions of 0.1 to 0.2 μm , special means of confining carriers within the laser cavity (including interspersed oxide or semiconductor layers), strained layers that reduce losses due to Auger recombination, and small, precise lateral dimensions that provide quantum wells to limit the number of allowable states within the cavity [1-4].

Three material systems are generally used for lasers with wavelengths between 650 and 1550 nm, as shown in Table 1.

TABLE 1
MATERIALS FOR LASERS BETWEEN 650 AND 1600 NM

Material Combination	Wavelength Range (μm)
AlGaAs/GaAs	650 - 850
InGaAsP/InP	1100 - 1600
*InGaAs/GaAs	900 - 1100

Manuscript received July 17, 2001. The research in this paper was carried out by the Jet Propulsion Laboratory, California Institute of Technology, under contract with the National Aeronautics and Space Administration, Code AE, under the NASA Electronic Parts and Packaging Program (NEPP).

A. H. Johnston, T. F. Miyahira and B. G. Rax are with the Jet Propulsion Laboratory, California Institute of Technology, Pasadena, CA, 91109.

The oldest material system is AlGaAs-GaAs, used for wavelengths between 650 and 850 nm. Alloys of AlGaAs are lattice matched with GaAs to about 0.1%, allowing a wide range of compositions to be used.

The second material system is InGaAsP-InP. This combination also allows good lattice matching for various compositional variations, and is widely used for wavelengths between 1100 and 1600 nm.

Close lattice matching is not possible for the wavelength "gap" between 850 and 1100 nm. Lasers within that region are made with InGaAs-GaAs, where there is a large amount of lattice mismatch (up to 3%). Thus, lasers fabricated with this material contain strained layers that must be restricted in thickness in order to avoid lattice defects that would degrade efficiency and reliability. Strained layers can be made with dimensions up to approximately 100 μm [5,6].

A diagram of an advanced laser diode is shown in Figure 1 (the top and bottom electrical contacts are not shown). The structure includes double-heterojunctions that allow carrier injection over very short distances, and lateral confinement using an oxide layer to restrict carrier injection from the top contact. For this material, the difference in refractive index between the GaAs and AlGaAs regions is sufficient to confine photons to the active region, but some lasers add additional layers that surround the active region for better optical confinement. Several methods can be used for lateral confinement, including ridge structures. Many variations in laser structure are possible, as discussed in References 1-7.

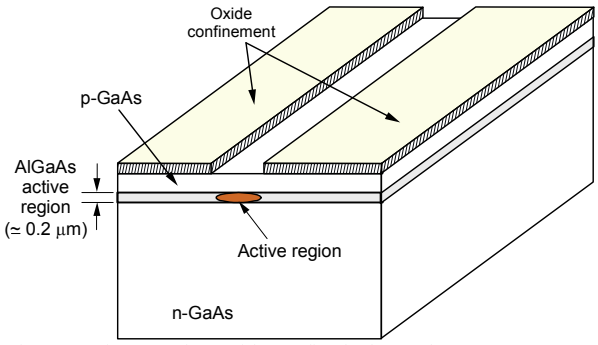

Figure 1. Diagram of an oxide-confined AlGaAs laser.

Proton displacement damage has been studied in only a few types of laser diodes [8-11] and little information is available on damage in more advanced devices. This paper compares proton damage in six different types of lasers, with wavelengths from 650 to 1550 nm, encompassing all three material systems discussed above. The lasers represent a broad range of current laser technologies. One

of the devices is a vertical cavity surface-emitting laser (VCSEL) that provides light output from the top surface, and uses a distributed Bragg reflector in combination with lateral oxide confinement in order to obtain high efficiency and low threshold current [12]. Some properties of these devices are listed in Table 2.

TABLE 2
WAVELENGTH AND THRESHOLD CURRENT OF LASERS IN THE STUDY

Manuf.	Part Type	λ (nm)	Threshold Current (mA)	Output Power (mW)	Slope Efficiency (mW/mA)	Active Layer	Construction
Lumex	LDP65001	650	20	5	0.33	GaAs/AlGaAs	
Honewell	SV5637	850	5	0.6	0.1	GaAs/AlGaAs	VCSEL
EG&G	C86135	905	46	25	0.80	InGaAs	Strained QW
Fermionics	LCX-1310	1310	10	5	0.17	InP/GaInAsP	Strained QW
Lumex	LDC13001	1300	12	5	0.35	InP/GaInAsP	
Mitsubishi	ML976H11	1550	15	6	0.25	InP/InGaAs	Distr feedback laser

Some devices had internal monitor diodes that are typically used as part of a feedback circuit to control operating conditions. Monitor diode degradation is an important consideration for many laser diode applications.

Two of the devices -- the EG&G 905 nm laser and the Mitsubishi 1550 nm laser -- were extremely expensive, and consequently tests were done on only four samples of those devices. Much larger test samples were used for tests of the other four laser types.

II. EXPERIMENTAL PROCEDURE

Previous work on laser diodes has shown that proton-induced damage is stable for long time periods for devices that are unbiased, but that considerable annealing occurs when devices are biased after (or during) irradiation because of recombination-enhanced annealing, even at room temperature [9,11,13]. Thus, in order to study the damage that results just after irradiation it is important to carefully control and limit the amount of current and time (essentially charge) that flows through the device after irradiation. Lang and Kimerling demonstrated that recombination-enhanced annealing depends on current at low injection levels, but saturates at higher injection levels (about 1 A/cm^2 for their samples, which represent much older laser technologies) [13]. Annealing of proton-induced damage in more advanced laser diodes was also reported by Zhao, et al. [11].

Devices were irradiated at UC Davis using 50-MeV protons. Irradiations were done with all pins grounded. Optical power and electrical measurements were made between successive irradiation steps. All measurements were done at 25 ºC. The measurement sequence was designed to limit measurement time and current to minimize recombination-enhanced annealing.

Optical measurements were made to determine the dependence of optical power on current, as well as the optical power from the internal monitor diode (when applicable). An external photodetector was used to measure optical power. A silicon photodiode was used for wavelengths below 950 nm. An InGaAs photodiode was used for longer wavelengths. The characterization included optical performance at currents well below the lasing threshold (where lasers function as LEDs) as well as at currents above the threshold. An Agilent Technologies 4156B parameter analyzer was used. The pulse width of the current forcing module was set to 80 μs, with fixed measurement ranges (this eliminates autoranging and precisely controls the measurement sequence). The total charge through the laser was less than 30 μC for each measurement set. Special test fixtures were designed that provided precise mechanical alignment between the laser and the external photodiode used to measure optical output power. The lasers were mounted in a plate, using a thermoelectric cooler to control the temperature to 25 ± 0.05 ºC. Measurement precision of optical power under fixed bias conditions was typically 1% or better.

III. EXPERIMENTAL RESULTS

Optical power and threshold current are two of the most critical laser diode parameters. The effect of proton damage on output power is shown for the Mitusbishi 1550 nm laser in Figure 2 where current in the external optical detector is plotted as a function of forward current in the laser before and after irradiation. For this device there is a very sharp transition between the LED mode (at forward currents below the "knee") and the laser mode, and the main effect of the radiation damage is a shift in threshold current. Note that the slope efficiency -- defined as the slope of the output power above the threshold current

Figure 2. Threshold current degradation of the Mitsubishi 1550 nm laser.

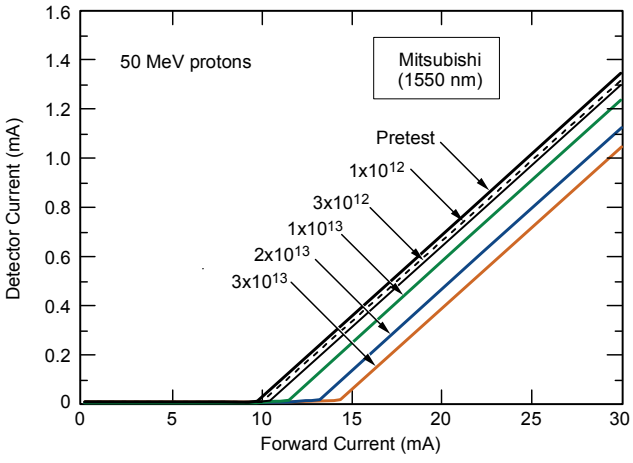

region -- is essentially unchanged after irradiation. Most earlier work on semiconductor lasers has shown similar results; i.e., nearly constant slope efficiency (until extreme degradation occurs). There was some variability in damage between different units of the same type. The coefficient of variation (σ/mean) was 0.12 to 0.2 for the various types of lasers used in our study.

The transition region of the Mitsubishi laser can be seen more clearly in Figure 3, which shows the data of Figure 2 on a semi-logarithmic plot. Note the sharpness of the transition region between the LED and laser operating modes.

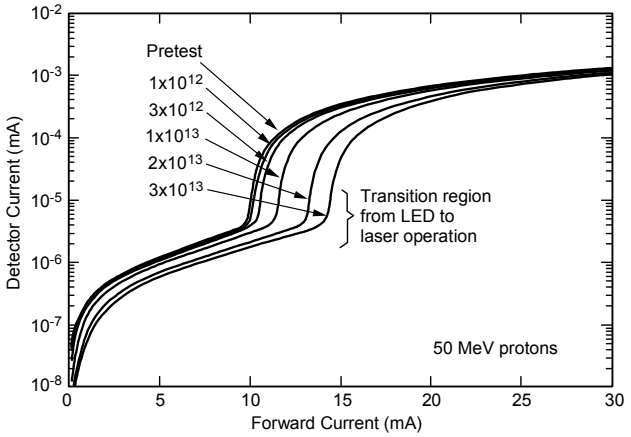

Figure 3. Degradation of the Mitsubishi 1550 nm laser plotted semi-logarithmically.

Not all laser diodes exhibit such ideal characteristics after irradiation. Figure 4 shows the effect of proton damage on the Lumex 650 nm laser. Two features should be noted. First, the slope efficiency changes; a significant change in slope efficiency occurs even after the first radiation level where the threshold current changes by only about 2%. Second, this device exhibits a more gradual transition between the LED and lasing modes compared to the Mitsubishi laser diode of Figure 2.

Figure 4. Degradation of light output of the Lumex 650 nm laser showing

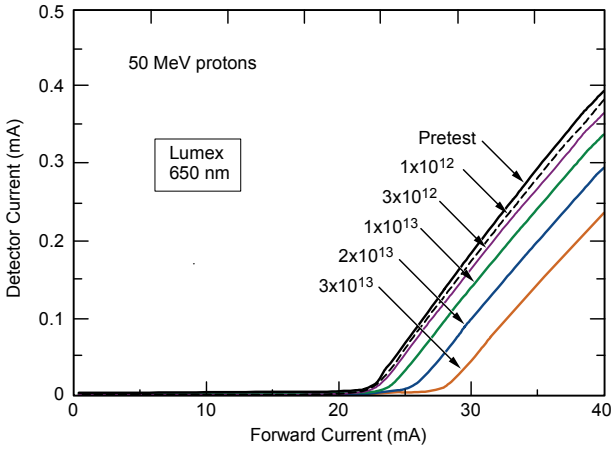

change in slope efficiency and "softening" of the transition region between LED and laser operating modes.

This transition region for the Lumex laser extends over a much wider range of current after irradiation, which is shown more clearly by the semi-log plot of the same data in Figure 5. The gradual transition is most likely caused by emission from several different lasing modes, which has been observed in laser reliability studies [14].

Figure 5. Lumex 650 nm laser results in Figure 4 plotted logarithmically to show transition characteristics in more detail.

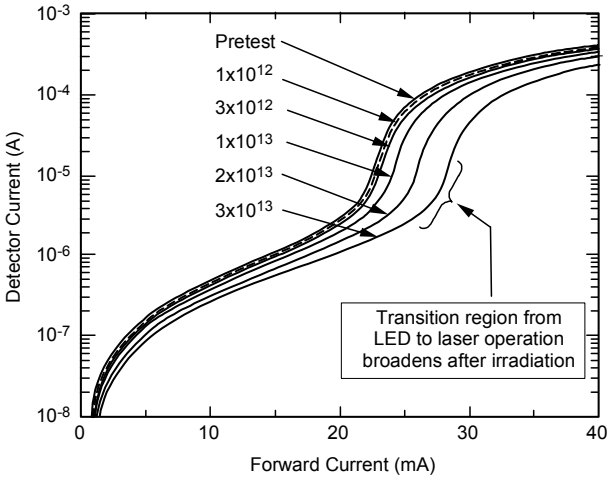

Another example of laser degradation is shown in Figure 6 for the EG&G strained quantum well laser. The slope efficiency of this device is much higher just after the device reaches threshold, but it decreases when the forward current is raised by just a few percent above the threshold current. That characteristic was not observed for any of the other lasers.

Figure 6. Threshold current degradation of the EG&G 905 nm laser diode.

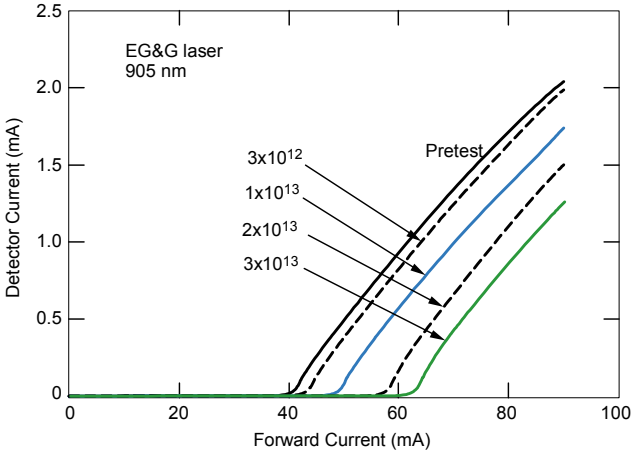

Figure 7 shows a semi-logarithmic plot of the data in Figure 6, which reveals several additional details. First, the transition region between LED and laser operation becomes more gradual after irradiation, just as for the 650 nm laser in Figure 4. Second, there is considerably more degradation at low injection (LED mode) compared to the other lasers. For I_F = 35 mA the light output decreases by about an order of magnitude after the highest radiation

level. This implies that a relatively large number of bulk defects are present after irradiation. However, much smaller relative changes occur in threshold current when the device enters the lasing mode. This suggests that different mechanisms dominate loss characteristics in the LED and laser modes. Loss mechanisms are discussed further in Section V.

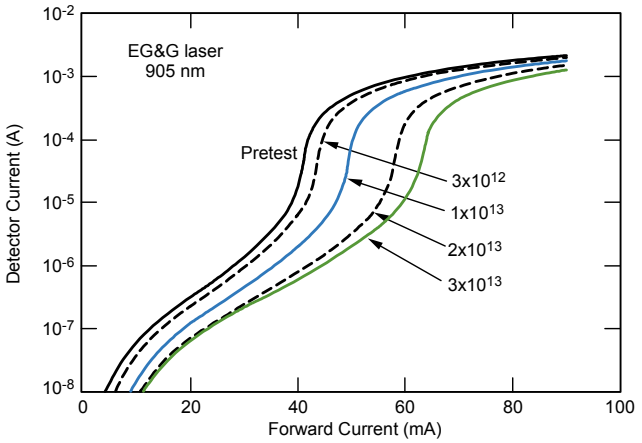

Figure 7. Semilogarthimic plot of the results for the EG&G laser in Figure 6.

VCSELs are very different from the other five types of lasers. VCSELs do not have constant slope efficiency (even prior to irradiation) because the small active region, which has a high thermal resistance, heats up significantly at high currents [9]. VCSEL power curves may also exhibit substructure because of variations and mismatch in the many layers that make up the internal Bragg reflector, which can cause the number of modes to vary with input power. Kinks in the optical power dependence on forward current are commonly observed in VCSEL structures [15].

Optical power characteristics of a typical Honeywell VCSEL before and after irradiation are shown in Figure 8. In this example there is substructure in the slope efficiency after irradiation that is probably related to differences in mode structure within the laser.

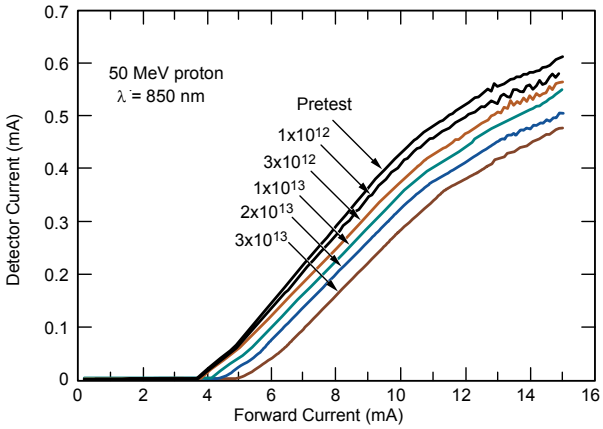

Figure 8. Degradation of light output of the Honeywell VCSEL.

Some VCSELs exhibited discontinuities (steps) in the output power characteristics prior to irradiation that were usually less pronounced after irradiation. Those steps usually occurred at currents well above the threshold current, and may be caused by a slight mismatch in the periodicity of the Bragg reflecting structure that increases the threshold current for some of the optical modes. Devices with large steps in output power were considered to be anomalous devices, and were not included in the set of devices that was used for radiation damage studies.

Threshold current changes after irradiation in the Honeywell VCSELs are somewhat larger than those reported by Barnes, et al. for a VCSEL with the same wavelength, manufactured by Sandia National Laboratories [16]. However, our tests were done at a lower energy (50 MeV instead of 192 MeV) and used a measurement sequence that was designed to limit annealing. The earlier data was taken with devices biased during irradiation, which decreases the damage because of annealing.

IV. Recombination-Enhanced Annealing

A. Basic Considerations

All of the laser diodes exhibited recombination-enhanced annealing. This can create severe difficulties during experiments that are intended to evaluate damage unless the operating conditions are carefully controlled, both during and after irradiation. Less damage will occur in devices that are operating during irradiation. However, it is difficult to make comparisons of biased and unbiased irradiation results because of the interplay between operating current and damage, and uncertainty about how to relate experiments done for relatively short times with bias to longer, less intense irradiations that occur in space. In this study we elected to irradiate devices without bias, and then evaluate annealing separately.

Annealing in laser diodes is difficult to evaluate because lasers operate at high power densities. Thus, measuring device properties after irradiation will inadvertently cause some of the damage to anneal. Therefore it is important to use pulsed measurements and also limit the current and time period in which all measurements are made after irradiation. For example, annealing is readily apparent for laser samples where they are operated above threshold for about one minute in order to measure wavelength with a spectrometer.

B. Annealing in Unbiased Devices

We performed isochronal annealing experiments on some of the irradiated samples in order to determine the temperature where thermal annealing -- without bias applied -- started to become important. The highest temperature used was 220 ºC (the maximum temperature available with standard ovens in our laboratory). Changes in threshold current were less than 2% during those tests. This is consistent with annealing results for proton damage in GaAs solar cells, which showed minimal annealing at

temperatures below 250 ºC [17]. Because such high temperatures are required for thermal annealing it appears unlikely that thermal annealing takes place in these laser diodes when annealing experiments are done using current within the normal operating range with the case temperature at 25 ºC. Note however that annealing in neutron-irradiated samples can occur at far lower temperatures (see Gill, et al. [18]). This difference in annealing properties is probably due to the difference in microscopic damage structure between neutrons and protons.

C. Annealing with Bias Applied

One case of interest is the situation where radiation damage has caused the threshold current to increase to the point where the operating current is no longer sufficient to drive the device into the lasing mode. Figure 9 shows annealing of the EG&G 905 nm laser after radiation damage has caused the threshold current to increase from 42 to 66 mA. Current in a detector is shown (with a forward current of 50 mA applied to the laser during measurement). The same electrical condition was used during annealing, forcing 50 mA through the device for several hours after irradiation. This experiment shows how the laser would recover if the bias current was set to a fixed condition that was insufficient to overcome the degradation in threshold current after irradiation. In order to interpret this figure one should note that current in the external detector (the Y axis) when the device is in the lasing mode is about 1 mA, more than two orders of magnitude above the detector current in the LED mode after it has been damaged by radiation. Thus, annealing is taking place at a far lower *optical* power density after the device degrades even though the electrical power density is unchanged. After the annealing period, the threshold current decreased from 64 mA to 56 mA. Although 50 mA is still well below the post-radiation threshold current, the optical power begins to increase sharply during annealing because the device is entering the transition region between LED and laser operation. This suggests that annealing is affected by optical power density as well as electrical power density.

Figure 9. Annealing of a 905 nm laser diode with current applied that is below the post-irradiation threshold current.

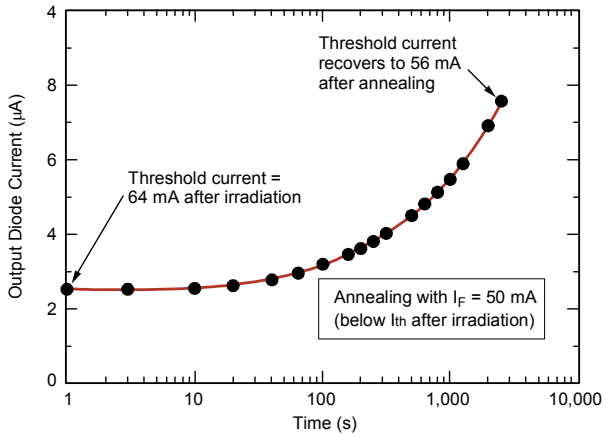

Results of an experiment to determine how annealing varied with different injection conditions are shown in Figure 10 for 1300 nm laser diodes from Lumex. The ordinate shows how the initial change in threshold current (relative to the pre-irradiation value) recovers after irradiation. Four different conditions are shown: an unbiased sample (except for post-radiation measurements done with very short pulses), a sample biased at 5 mA, below the lasing threshold (open symbols), and two devices that were biased above the lasing threshold (solid symbols). Note that the damage is essentially unchanged for the unbiased device, even after about a one-month time period. In contrast, damage in the other samples that are continuously biased gradually diminishes with time.

Figure 10. Dependence of annealing of 1300 nm laser diodes on injection conditions. Samples were held at a constant temperature, 25 ºC, during the annealing period.

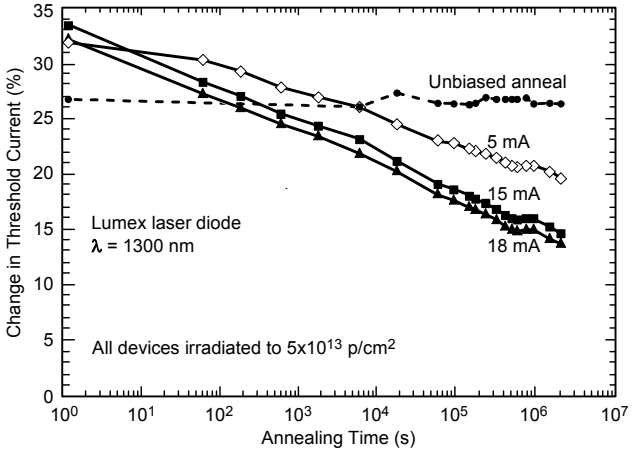

Annealing in LEDs at different currents depends on the total injected charge after irradiation [19], with a charge threshold of about 0.001 coulomb. That is, recombination-enhanced annealing in LEDs starts to become significant at about 1 mC, and progresses until the total charge is 1000 C or more. Our initial experiments indicate that annealing in laser diodes also depends on total charge, with comparable sensitivity to total charge after irradiation. However, it is more difficult to make comparisons between different types of lasers because of differences in geometry and material type. For example, the EG&G laser is designed with a very small cavity, nominally 1 x 3 μm, resulting in a much larger optical power density compared to LEDs.

Note further that although injection-enhanced annealing is quite significant for amphoterically doped LEDs, double-heterojunction LEDs exhibit only slight damage recovery, even after 1000 C of charge [19]. The doping levels and materials used in double-heterojunction LEDs are very similar to those used in laser diodes. The reason for the increased sensitivity of laser diodes to annealing may be

due to the much higher optical power densities that are present in lasers, and the requirement for high internal optical gain, neither of which occurs in LEDs.

We also investigated injection-dependent annealing in the 850 nm VCSELs. Those results are shown in Figure 11. Annealing in the VCSELs occurred much more rapidly than for conventional laser structures. When the device was operated below threshold (the 1 mA data in the figure) the time period for recovery was about four orders of magnitude longer than when the VCSELs were operated in the lasing mode.

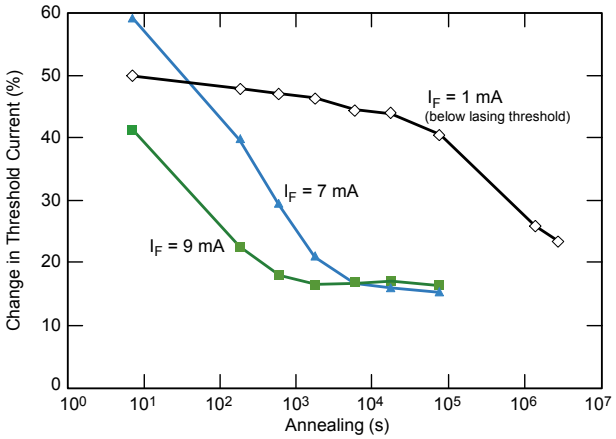

Figure 11. Dependence of annealing on injection conditions for the Honeywell VCSEL devices.

When the VCSELs were annealed in the lasing mode they recovered much faster than conventional lasers. However, the time required for damage recovery for the 1 mA condition (well below threshold) was comparable to the time required for annealing in the other laser diode structures.

C. Monitor Diode Degradation

Many applications rely on current from an internal monitor diode to provide input to a feedback circuit that is designed to control the laser power output within a narrow range. The monitor diodes are usually placed to the side of the device, reflecting a small amount of light from the exit window to the monitor diode.

Figure 12 shows degradation of monitor diodes for two of the lasers, along with degradation of a typical silicon photodiode. For the 1300 nm laser, degradation in the photodiode is much greater than degradation in the laser, which could have a serious impact on applications that rely on the internal diode responsivity to control current in the laser. The internal diode in the 650 nm laser is significantly harder. Note also that degradation of the monitor diodes will anneal very little compared to annealing in the laser diodes because they operate at very low currents.

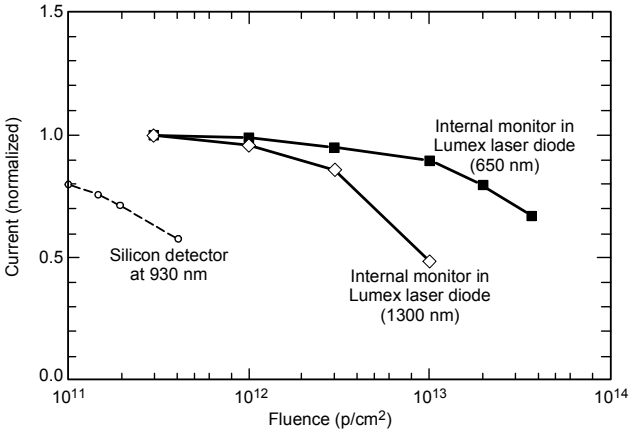

Figure 12. Degradation of internal monitor photodiodes of the two lasers manufactured by Lumex.

Degradation of a typical silicon p-n silicon detector is also shown in Figure 11 for comparison. The III-V detectors used for internal monitor diodes are far less sensitive to displacement damage than silicon detectors, which is expected because charge collection in direct-bandgap semiconductors does not require long minority carrier lifetime [20].

V. Discussion

A. Damage in the Different Types of Lasers

In addition to measuring electrical and optical power, measurements of wavelength and spectral width were made with a spectrometer before and after irradiation for some of the samples. The spectral width of the various lasers was typically 6 to 15 nm (compared with 60-90 nm for LEDs), and changes in spectral width were less than 0.2 nm after irradiation provided that the measurements were made well above the threshold current. The spectral width increases for *constant drive* conditions if radiation damage increases the threshold current to the point where the laser operates near threshold, but the same increase in spectral width is also seen in unirradiated devices when the forward current is just above threshold. Thus, we conclude that radiation damage has little or no effect on wavelength and spectral width, although that conclusion may not apply to lasers that are designed with very narrow spectral width. The same temperature controlled fixture was used for wavelength measurements, which is an important detail because of the dependence of wavelength on temperature.

Even though threshold current is not the only parameter of interest, it remains one of the most important parameters for characterizing radiation degradation. Earlier experimental work showed that the change in threshold current change after irradiation was linearly dependent on proton or neutron fluence [8-11]. Four of the laser diodes in our study -- including the VCSEL -- also behaved linearly, as shown in Figure 13. These data are mean values of six different units of each type, measured just after irradiation with a series of pulsed measurement to reduce the effects of recombination-enhanced annealing.

Figure 13. Dependence of threshold current change on fluence for laser diodes with linear damage relationships.

The other two laser diode types had nonlinear

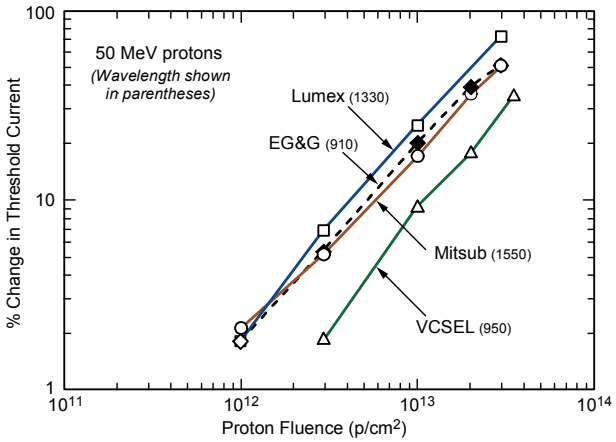

relationships between threshold voltage change and fluence. Those results are shown in Figure 14; the dashed line shows a linear slope for comparison. The nonlinear behavior was consistent among different samples of the same laser type, not atypical behavior of one or two units. This nonlinear dependence is important because it makes it more difficult to compare laser damage under different conditions or fluences.

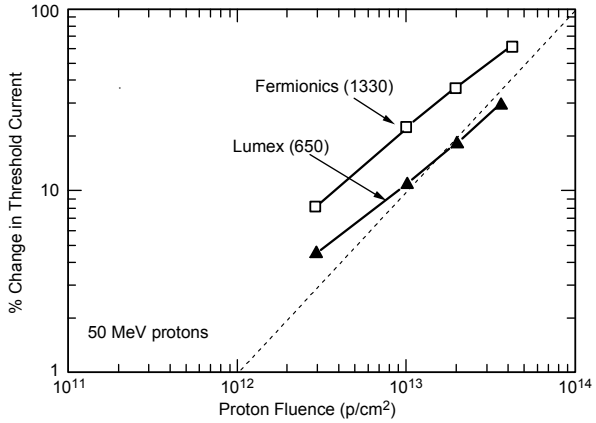

Figure 14. Dependence of change in threshold current on fluence for the Lumex 650 nm and Fermionics 1300 nm lasers.

Reasons for the nonlinear behavior are discussed in the next subsection. Note that both types of lasers with nonlinear behavior had more gradual transitions between the LED and laser operating modes compared to the other four lasers that had sharp transition regions (and linear fluence dependence). Note also that the 1300 nm laser from the other manufacturer exhibited linear behavior, suggesting that damage nonlinearity is not just due to the different material technologies.

One unexpected result is that the fluence required for moderate increases in threshold current -- 20 to 30% -- varied by about a factor of two for all six of the laser types, even though they use different materials and construction.

There were much larger differences in the way that the different laser types behaved in the *LED mode* (below the lasing threshold). For constant drive current, the optical power output in the LED mode changed by as little as a factor of 2 (for the 1550 nm laser) to more than a factor of 10 (for the EG&G 905 nm laser). This suggests that fundamental differences in damage sensitivity that affect the devices at low injection are unimportant when they operate as lasers.

B. Laser Theory

Below the threshold region lasers behave like light-emitting diodes. Under very low injection conditions, injected carriers recombine because of bulk defects or surface recombination, and no light is produced. As the injection level increases, radiative recombination becomes the dominant recombination process and the LED (or laser) begins to produce photons, operating as an LED. The transition between these regions is marked by a change in the slope of the forward-voltage and current (which ideally changes by a factor of 2) [21]. These recombination processes can be described as

$$R = R_{surf} + R_{bulk} + R_{sp} \quad (1)$$

where R is the total recombination rate, R_{surf} is the surface recombination term, R_{bulk} is the bulk recombination term, and Rsp is the spontaneous (radiative) recombination term.

For lasers, we have to add two additional terms to Equation 1 [6,7,14]. The first is an additional radiative recombination term, R_{stim}, which is the result of stimulated emission from the high optical carrier density that is present during laser operation. Unlike spontaneous recombination, stimulated recombination produces photons that have the same wavelength and direction as the internal photons that cause the stimulated emission process. This is the dominant recombination mechanism in semiconductor lasers when they are operated in the lasing mode. We also have to add an Auger recombination term (R_{Auger}) because of the high carrier density (Auger recombination is negligible for LEDs because of the low carrier density). Recombination in lasers can be expressed as

$$R = R_{surf} + R_{bulk} + R_{Auger} + R_{sp} + R_{stim} \quad (2)$$

The threshold condition for a laser requires that the injected carrier density is high enough to overcome the first three (loss) terms on the right side of Equation 2 as well as the spontaneous recombination term; laser operation requires that the stimulated recombination term dominates.

The various terms in Equation 2 have different dependences on carrier density, N. Studies of surface and bulk recombination have shown that those terms are generally proportional to carrier density. Auger recombination depends on N^3, and the spontaneous

recombination rate depends on N^2. Thus, (2) can be written in the form

$$R = AN + BN^2 + CN^3 + R_{stim} \qquad (3)$$

where A, B and C are constants. Ignoring the cubic (Auger) term† and assuming the first term is small (valid before radiation damage), the carrier density must be high enough to overcome recombination from the second term, which represents spontaneous (radiative) recombination that competes with stimulated recombination. Once the carrier density exceeds that value, stimulated recombination dominates. This threshold condition for laser operation can be estimated from measurements of the bimolecular recombination coefficient, B, which have been studied for all three of the materials used for the lasers in this work; typical values of B are 1.2 x 10^{-10} cm^3/s for GaAs, and 0.7 x 10^{-10} cm^3/s for AlGaAs [22].

The threshold current I_{th} depends on physical factors in addition to carrier recombination, as shown by Equation 4 below [1,3,5]

$$I_{th} = \frac{qVBN_{tr}^2}{\eta_i} e^{2<\alpha i>\Gamma g} \qquad (4)$$

where q is electronic charge, V is the volume of the laser cavity, B is the bimolecular recombination coefficient for bulk recombination, N_{tr} is the carrier density at threshold (transparency condition), η_i is the internal quantum efficiency, α_i is the transverse mode loss (which competes with the longitudinal modes), Γ is the transverse mode confinement factor, and g is the cavity gain. To first order, the threshold current depends on the square of the injected carrier density.

The cavity gain, g, is a nonlinear function of N, and it is possible to overcome internal nonradiative recombination loss terms (such as bulk or surface recombination) by increasing the carrier density to the point where the increased cavity gain compensates for the additional recombination losses, allowing efficient laser operation even after additional defects have been created.

- - - - -

†Auger recombination is negligible for GaAs/AlGaAs lasers, but is an important contribution for InGaAsP/InP lasers [23].

Damage linearity depends on the relationship between cavity gain and carrier density of the material, which is approximately logarithmic [24]. Therefore damage is expected to be linear over a restricted range of conditions. When the threshold current increases by 40%, the damage begins to become noticeably sublinear with fluence if the logarithmic dependence of gain on carrier density applies. That is in reasonable agreement with our results, as well as with older results for neutron damage in laser diodes [25].

Parametric curve fits for the dependence of gain on N and current density have been compiled by Coldren and Corzine and others which are sufficiently accurate for laser design [3,7]. For small changes in threshold voltage, the slope is approximately 3 for bulk GaAs, but is 4.5-6 for strained layers using InP. This sensitivity of gain to carrier density explains why the more extreme degradation of laser diodes at low injection (LED mode) does not result in very large increases in threshold current.

Material properties also affect laser degradation. Although the gain of InP-based lasers (such as the 1550 nm devices) is considerably higher than that of GaAs-based lasers, Auger recombination losses are much higher in InP. This causes the output power at low injection (below threshold) to increase sublinearly with increasing current, whereas the relationship is linear for materials with low Auger coefficients. It also affects the relationship between threshold current and carrier density.

In addition to the increase in bulk recombination, radiation defects also cause carrier removal. For GaAs and related III-V devices, carrier removal rates are typically between 300 and 500 cm^{-1} [26]. Carrier densities in semiconductor lasers can be estimated from the value of the bimolecular coefficient, B, as well as the other parameters in Equation 1. Typical values are 2-4 x 10^{18} cm^{-3}, which are also verified by processing data from the literature [2-6]. This suggests that carrier removal effects may begin to become important at radiation levels above about 2 x 10^{13} p/cm^2, which may also contribute to nonlinear damage at high fluences. However, at lower fluences carrier densities should change by less than 1%.

C. Measurement and Characterization

Characterization of laser diode damage is considerably more complex than that of characterizing light-emitting diodes for many reasons. First, this study included lasers with different composition and structure. Second, the specific geometry of a laser can have a pronounced effect on threshold current and output power characteristics, and these factors have to be sorted out in order to make meaningful comparison between different types of lasers, particularly for VCSELs which operate under much different conditions than conventional lasers.

Although threshold current is clearly important, measurement of the optical power characteristics over a wide range of currents can provide insight into damage mechanisms, including the importance of Auger recombination. Because annealing is so strongly dependent on injection conditions, measurements need to be carefully set up to limit the time and current (essentially total charge), otherwise the measurements will inadvertently cause a significant amount of the damage to anneal,

underestimating the effects of radiation on device performance.

Lifetime measurements can also be made on laser diodes, although modern lasers require measurements at frequencies above 1 GHz, which are difficult to make. A revised approach has been developed by Schtengel, et al., which allows lifetime to be measured from electrical characteristics [27], eliminating the need for high-speed optical power measurements. However, lifetime in laser structures changes rapidly with injection level, and is of limited value in analyzing damage to devices that are functioning in the lasing mode, where nearly all of the injected carriers recombine [23,24,28].

VI. Conclusions

This paper has investigated proton damage in several types of laser diodes. The lasers that were tested cover a wide range of wavelengths and included three different material types. One surprising result was that the sensitivity of the devices to proton damage was within about a factor of two for all six types of laser diodes in spite of the different materials and fabrication methods. This was explained by noting the

The parameters that are most affected by radiation damage are threshold current and slope efficiency. For most lasers, threshold current increases linearly with fluence provided the relative increase is less than about 40%, in agreement with theoretical predications assuming that bulk recombination is the dominant mechanism for radiation degradation. Nonlinearities are expected at higher levels because of the nonlinear relationship between carrier density and cavity gain, as well as from carrier removal effects that may also become important for fluences above approximately 3 x 10^{13} p/cm^2. Measurement of laser characteristics below the threshold level, where they operate as LEDs, can provide additional information about degradation mechanisms.

Recombination-enhanced annealing is an important factor for all of the lasers in the study, unlike LEDs that are fabricated with similar material technologies. The reason for the difference is the requirement for high gain and low recombination within the laser cavity when the laser operates in the lasing mode. Experimental measurements have to be carefully planned to avoid interference from annealing, which will underestimate the amount of damage in cases where lasers operate with low duty cycle pulses.

The effect of displacement damage on wavelength is minimal, changing the wavelength by less than 0.2 nm for all of the lasers in our study. However, this conclusion does not necessarily apply to lasers that are designed with very narrow bandwidths. Lasers of that type were not included in our study.

Finally, we used 50 MeV protons in our study because there is better agreement about how NIEL calculations agree with experimental results at that energy compared to results at higher energy. Although energy dependence of damage in laser diodes is an important topic, it is beyond the scope of the present work.

References

[1] D. Ahn and S. L. Chuang, "Optical Gain in a Strained Quantum Well Laser," IEEE J. Quant. Elect., **24** (12), pp. 2400-2406 (1988).

[2] R. J. Fu, C. S. Hong, E. Y. Chan, D. J. Booher and L. Figueroa, "High Temperature Operation of InGaAs Strained Quantum-Well Lasers," IEEE Phot. Tech. Lett., **3**(4), pp.308-310 (1991).

[3] C. H. Lin and Y. H. Ho, "Empirical Formulas for Design and Optimization of 1.55 μm InGaAs/InGaAsP Strained Quantum Well Lasers," IEEE Phot. Tech. Lett., **5**(3), pp. 288-290 (1993).

[4] A. C. Crook, M. L. Osowski, G. M. Smith, J. Frame, M. Grupen and T. A. DeTemple, "A Universal Optical Heterostructure for Photonic Integrated Circuits: A Case Study in the AlGaAs Material System," IEEE J. of Selected Topics in Quantum Electronics, (**2**)2, pp. 341-347 (1996).

[5] K. Nakahara, K. Uomi, T. Tsuchiya, A. Niwa, T. Haga and T. Taniwatari, "1.3-μm InGaAsP-InP Modulation-Doped Strained Muliquantum-Well Lasers," IEEE J. of Selected Topics in Quantum Electronics, (**3**)2, pp. 166-172 (1997).

[6] J. J. Coleman, "Strained Layer InGaAs Quantum-Well Heterostructure Lasers," IEEE J. of Selected Topics in Quantum Electronics, (**6**)6, pp. 1008- 1012 (2000).

[7] L. W. Coldren and F. W. Corzine, *Diode Lasers and Photonic Integrated Circuits*, New York: John Wiley, 1995.

[8] H. Lischka, H. Henschel, O. Kohn, W. Lennartz and H. Schmidt "Radiation Effects in Light Emitting Diodes, Laser Diodes, Photodiodes and Optocouplers," RADECS93 Proceedings, pp. 226-231.

[9] B. D. Evans, H. W. Hager and B. W. Hughlock, "5.5 MeV Proton Irradiation of a Strained Quantum Well Laser Diode," IEEE Trans. Nucl. Sci., **40**(6), pp.1645-1654 (1993).

[10] Y. F. Zhao, A. R. Patwary, R. D. Schrimpf, M. A. Neifeld and K. F. Galloway, "200 MeV Proton Damage Effects on Multi-Quantum Well Laser Diodes," IEEE Trans. Nucl. Sci., **44**(6), pp. 1898-1905 (1997).

[11] Y. F. Zhao, R. D. Schrimpf, A. R. Patwary, M. A. Neufeld, A. W. Al-Johani, R. A. Weller and K. F. Galloway, "Annealing Effects on Multi-Quantum Well Laser Diodes," IEEE Trans. Nucl. Sci., **45**(6) pp. 2826-2832 (1998).

[12] K. D. Choquette and H. Q. Hou, "Vertical-Cavity Semiconductor Lasers: Moving from Research to Manufacturing," Proc. IEEE, **85**,(11), pp. 1730-1739 (1997).

[13] D. V. Lang and L. C. Kimerling, "Observation of Recombination-Enhanced Defect Reactions in Semiconductors," Phys. Rev. Lett., **33**(8), pp. 489-492 (1974).

[14] I. Vurgaftman and J. R. Meyer, "Effects of Bandgap, Lifetime, and Other Nonuniformities on Diode Laser Thresholds and Slope Efficiences," IEEE J. of Selected Topics in Quantum Electronics, (**3**)2, pp. 475-484 (1997).

[15] G. Hasnain, K. Tai, L. Yang, Y. H. Wang, R. J. Fischer, J. D. Wynn, B. Weir, N. K. Dutta and A. Y. Cho, "Performance of Gain-Guided Surface Emitting Lasers with Semiconductor Distributed Bragg Reflectors," IEEE J. Quantum Electronics, **27**(6), pp. 1377-1385 (1991).

[16] C. E. Barnes, J. R. Schwank, G. M .Swift, M. G. Armendariz, S. M. Guertin, G. L. Hash, and K. D. Choquette, "Proton Irradiation Effects in Oxide-Confined Vertical Cavity Surface Emitting Diodes," Paper L-O-2, presented at the RADECS99 Conference, Abbaye de Fontervaud, France, September 13-17, 1999 (unpublished).

[17] B. E. Anspaugh, *GaAs Solar Cell Radiation Handbook*, Jet Propulsion Laboratory publication JPL96-9, July 1, 1996.

[18] K. Gill, C. Azevedo, J. Batten, C. Cervelli, R. Grabit, F. Jensen, J. Troska and F. Vasey, "Aging Tests of Radiation Damaged Lasers and Photodiodes," RADECS99 Proceedings, IEEE Doc. 99TH847, pp. 429-436.

[19] A. H. Johnston and T. F. Miyahira, "Characterization of Proton Damage in Light-Emitting Diodes," IEEE Trans. Nucl. Sci., **47**(6), pp. 2500-2507 (2000).

[20] S. L. Chuang, *Physics of Optoelectronic Devices*, New York: John Wiley, 1995.

[21] P. F. Lindquist, "A New Model for Light Output Degradation of Direct Bandgap Semiconductors," 1980 International Reliability Physics Proceedings, pp. 145-150.

[22] R. F. Kazarinov and M. R. Pinto, "Carrier Transport in Laser Heterostructures," IEEE J. Quantum Electronics, **30**(1), pp. 49-53 (1994)

[23] T. Kallstenius, A. Landstedt, U. Smith and P. Granestrand, "Role of Nonradiative Recombination in the Degradation of InGaAsP/InP-Based Bulk Lasers," IEEE J. Quantum Electronics, (**36**)11, 1312-1322 (2000).

[24] T. A. DeTemple and C. M. Herzinger, "On the Semiconductor Laser Logarithmic Gain-Current Density Relation," IEEE J. Quantum Electronics, (**29**)5, 1246-1252 (1993).

[25] W. W. Chow and R. F. Carson, "Neutron Effects in High Power Laser Diodes," IEEE Trans. Nucl. Sci., **36**(6), 2076 (1989).

[26] A. B. Campbell, A. R. Knudsen, W. J. Stapor, G. Summers, M. A. Xapsos, M. Jessee, T. Palmer, R. Zuleey and C. J. Dale, "Particle Damage Effects in GaAs JFET Test Structures," IEEE Trans. Nucl. Sci., **33**(6), pp.1435-1441 (1986).

[27] G. E. Schtengel, D. A. Ackerman and P. A. Morton, "True Carrier Lifetime Measurements of Semiconductor Lasers," Elect. Lett., **31**(20). pp.1747- 1748 (1995).

[28] J. M. Pikal, C. S. Menoni, H. Temkin, P. Thiagarajan and G. Y. Robinson, "Carrier Lifetime and Recombination in Long-Wavelength Quantum-Well Lasers," IEEE J. of Selected Topics in Quantum Electronics, (**5**)3, pp.613-619 (1999).